Introducing [Mn(CO)$_3$(tpa-$\kappa^3 N$)]$^+$ as a novel photoactivatable CO-releasing molecule with well-defined iCORM intermediates - synthesis, spectroscopy, and antibacterial activity

Christoph Nagel,[a] **Samantha McLean,**[b] **Robert Poole,**[b] **Holger Braunschweig,**[a] **Thomas Kramer,**[a] **and Ulrich Schatzschneider***[a]

[a]Institut für Anorganische Chemie,

Julius-Maximilians-Universität Würzburg, Am Hubland, D-97074 Würzburg, Germany

Fax: +49 931 3184605

eMail: ulrich.schatzschneider@uni-wuerzburg.de

[b]Department of Molecular Biology and Biotechnology, The University of Sheffield,

Western Bank, Sheffield S10 2TN, UK

Supporting Information

Experimental

Synthesis of ligands and precursors. Tris(2-pyridylmethyl)amine (tpa) was synthesized from 2-picolylchloride hydrochloride and 2-picolylamine following the procedure of Tyeklár and Karlin.[1] Polymeric $[RuCl_2(CO)_2]_n$ was prepared from ruthenium trichloride trihydrate and paraformaldehyde in degassed formic acid according to White *et al.*[2]

Synthesis of $[Ru(CO)_2(tpa-\kappa^4N)](PF_6)_2$. $[Ru(CO)_2Cl_2]_n$ (500 mg, 2.2 mmol) and tris(2-pyridylmethyl)amine (725 mg, 2.6 mmol) were dissolved in degassed ethanol (30 mL) under argon and heated to reflux for 2 h. Then, a saturated solution of ammonium hexafluorophosphate in water was added to precipitate the product as a white solid, which was collected and recrystallized by diffusion of diethylether into a solution of the crude compound in acetone, leading to the formation of colorless crystals which were suitable for X-ray structure analysis. Yield: 50% (781 mg, 1.1 mmol). Elemental analysis (%): calc. $C_{20}H_{18}F_{12}N_4O_2P_2Ru$: C 32.58, H 2.46, N 7.60, found: C 33.88, H 2.47, N 7.91; IR (ATR, cm^{-1}): 3383 (m), 2095 (vs, C≡O), 2033 (vs, C≡O), 1614 (w), 1448 (w), 820 (vs), 763 (vs); ^1H NMR (acetone-d_6, 200.13 MHz): δ 9.40 (d, 1H, ^3J = 5.7 Hz, tpa-$H6$), 8.96 (d, 2H, ^3J = 5.7 Hz, tpa-$H6$), 8.17 (dt, 2H, ^3J = 7.8 Hz, ^4J = 1.5 Hz, tpa-$H5$), 8.04 (dt, 1H, ^3J = 7.9 Hz, ^4J = 1.4 Hz, tpa-$H5$), 7.93 (d, 2H, ^3J = 7.2 Hz, tpa-$H4$), 7.63 (m, 3H, tpa-$H4/3$), 7.50 (d, 1H, ^3J = 7.6 Hz, tpa-$H3$), 5.88 (d, 2H, ^2J = 16.1 Hz, CH_2), 5.67 (d, 2H, ^2J = 16.1 Hz, CH_2), 5.49 (s, 2H, CH_2); ^{13}C NMR (acetone-d_6, 50.32 MHz): δ 162.61 (tpa-$C2$), 162.45 (tpa-$C2$), 156.82 (tpa-$C6$), 153.20 (tpa-$C6$), 141.92 (tpa-$C5$ 2x overlapping), 127.70 (tpa-$C4$), 127.13 (tpa-$C4$), 126.28 (tpa-$C3$), 123.63 (tpa-$C3$), 71.82 (CH_2), 69.43 (CH_2), 2x M(C≡O) not detected; MS (ESI$^+$, CH$_3$CN): *m/z*: 455.0236 {(Ru(CO)(tpa-κ^4N)]Cl}$^+$, 483.0152 {[Ru(CO)$_2$(tpa-κ^4N)]Cl}$^+$, 593.0115 {[Ru(CO)$_2$(tpa-κ^4N)]PF$_6$}$^+$, 1330.9902 {[Ru(CO)$_2$(tpa-κ^4N)]$_2$(PF$_6$)$_3$}$^+$.
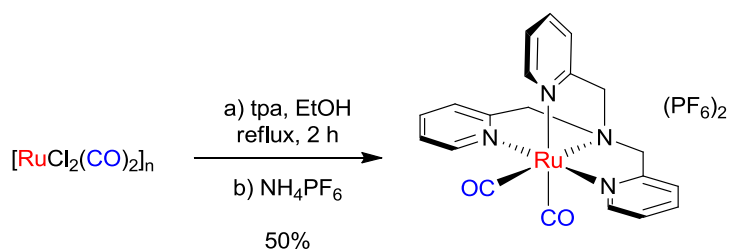
Scheme S1 Synthesis of $[Ru(CO)_2(tpa-\kappa^4 N)](PF_6)_2$ from $[Ru(CO)_2Cl_2]_n$ and tris(2-pyridylmethyl)amine (tpa) in degassed ethanol at reflux.

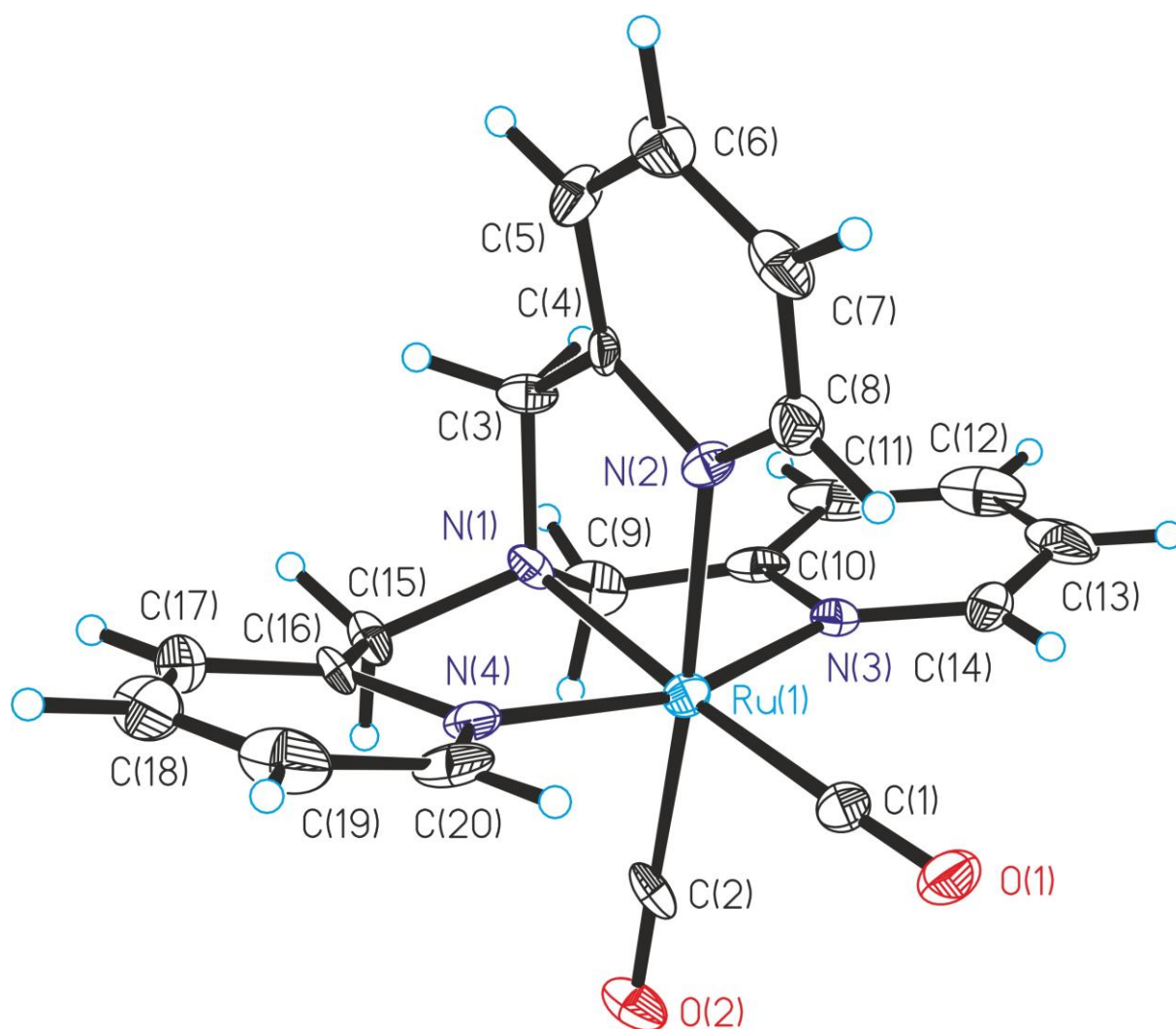**Figure S1** Molecular structure of $[Ru(CO)_2(tpa-\kappa^4 N)]^{2+}$ with ellipsoids drawn at the 50% probability level. The two hexafluorophosphate counterions are not shown for clarity.

Table S1 Crystallographic parameters for $[Ru(CO)_2(tpa\text{-}\kappa^4 N)](PF_6)_2$

Empirical formula	$C_{20}H_{18}F_{12}N_4O_2P_2Ru$
Formula weight (g·mol^{-1})	737.39
Temperature (K)	100(2)
Radiation, λ (Å)	$Mo_{K\alpha}$ 0.71073
Crystal system	Orthorhombic
Space group	$P2_12_12_1$
Unit cell dimensions	
a (Å)	11.967(6)
b (Å)	13.361(7)
c (Å)	15.789(7)
α (°)	90.00
β (°)	90.00
γ (°)	90.00
Volume (Å^3)	2525(2)
Z	4
Calculated density (Mg·m^{-3})	1.940
Absorbtion coefficient (mm^{-1})	0.866
$F(000)$	1456
Theta range for collection	2.00 to 26.02°
Reflections collected	18820
Independent reflections	4897
Minimum/maximum transmission	0.6437/0.7454
Refinement method	Full-matrix least-squares on F^2
Data / parameters / restrains	4897 / 352 / 78
Goodness-of-fit on F^2	1.054
Final R indices [I>2σ(I)]	$R_1 = 0.0603$, $w\text{R}^2 = 0.1327$
R indices (all data)	$R_1 = 0.0948$, $w\text{R}^2 = 0.1497$
Maximum/minimum residual electron density (e·Å^{-3})	1.603 / −1.519

Table S2 HOMO-3 to LUMO+8 of $[Mn(CO)_3(tpa-\kappa^3N)]^+$ calculated with BP86/TZVP. Isosurface values are plotted at ±0.05, with positive values shown in red and negative ones in blue.
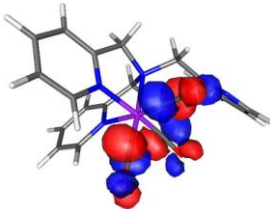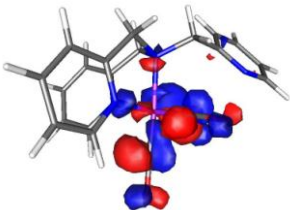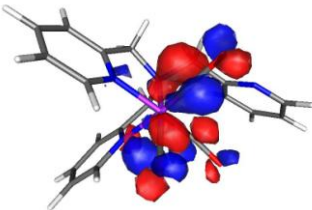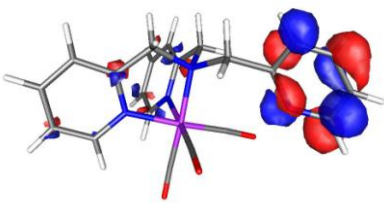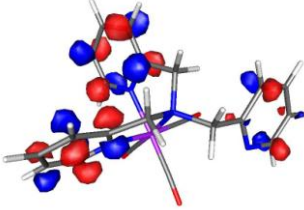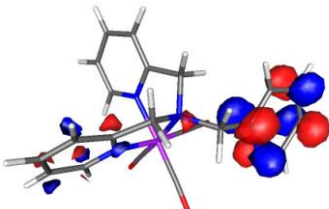
Orbital	Energy in eV (occupation)	Character	molecular orbital plot
118	0.3452 (0)	$\pi^*(CO)$	
117	-0.5004 (0)	$\pi^*(CO)$	
116	-0.5475 (0)	$\pi^*(py)$	
115	-1.0551 (0)	$\pi^*(py)$	
114	-1.2292 (0)	$\pi^*(py)$	
113	-1.3755 (0)	$\pi^*(py)$	

Table S2 continued
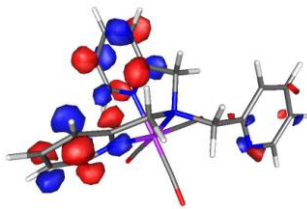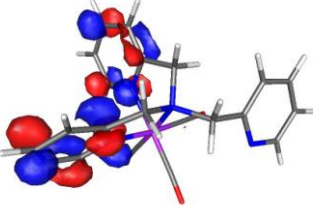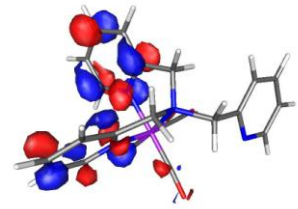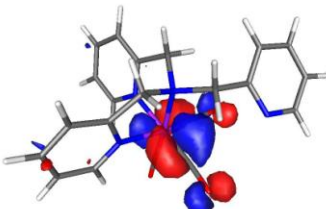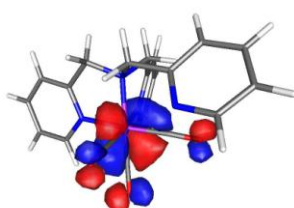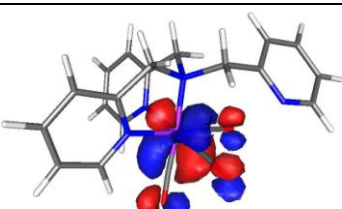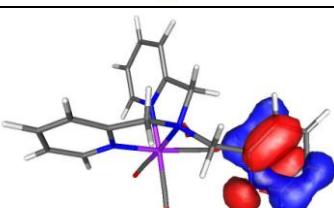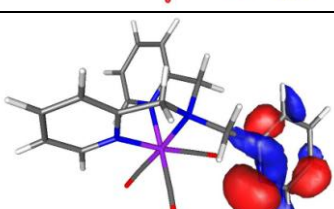
112	-1.7197 (0)	π^*(py)	
111	-2.1192 (0)	π^*(py)	
110 (LUMO)	-2.3659 (0)	π^*(py)	
109 (HOMO)	-6.2979 (2)	d(Mn)	
108	-6.6190 (2)	d(Mn)	
107	-6.6847 (2)	d(Mn)	
106	-7.4893 (2)	π(py)	
105	-7.5291 (2)	π(py)	

Table S3 TDDFT difference densities for the most important singlet excitations for $[Mn(CO)_3(tpa\text{-}\kappa^3N)]^+$ in the 230 to 600 nm range, calculated with B3LYP/TZVP. Isosurface values are plotted at ±0.002, with positive values shown in green and negative ones in red.
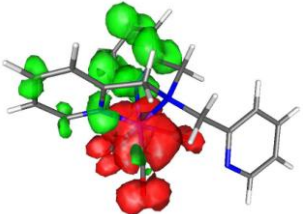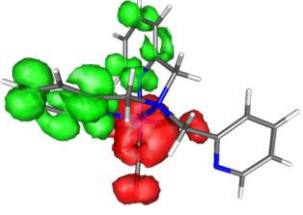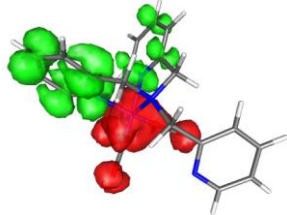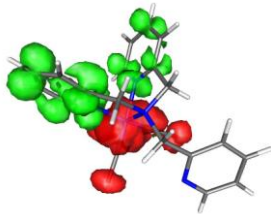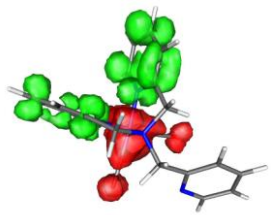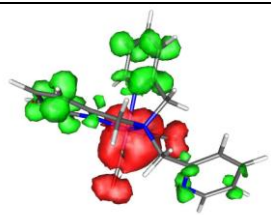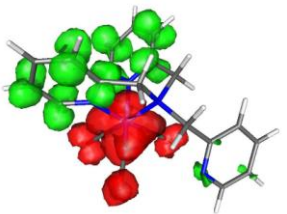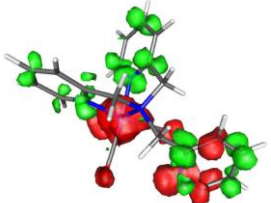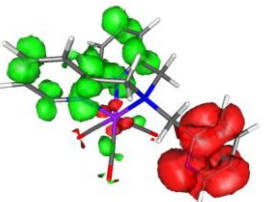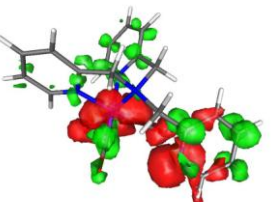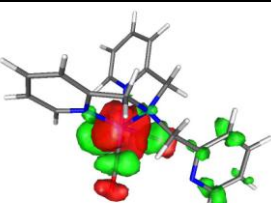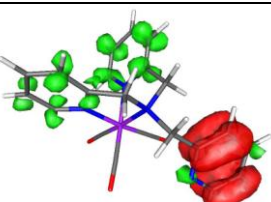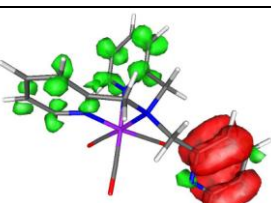
state	λ nm	f_{osc}	difference density plot
1	406.2	0.0340	
3	376.5	0.0609	
4	360.8	0.0805	
5	358.4	0.0736	
6	346.7	0.0617	
7	337.4	0.0119	
10	310.8	0.0139	

Table S3 continued

16	272.3	0.0145	
17	297.8	0.0130	
21	262.0	0.0109	
29	242.3	0.0133	
32	244.1	0.0799	
33	235.1	0.0193	

Model calculations on the effect of replacement of coordinated DMSO by water

In order to validate the approach of using coordinated water instead of DMSO to keep the computational demand acceptable in structures **B**, **B'**, **D**, and **D'**, very simple model systems, in which all nitrogen donor groups are replaced by ammine ligands were constructed and the calculations then repeated on $[Mn(CO)_3(NH_3)_3]^+$ as well as $[Mn(CO)_2(NH_3)_3(OH_2)]^+$, $[Mn(CO)_2(dmso\text{-}\kappa O)(NH_3)_3]^+$, and $[Mn(CO)_2(dmso\text{-}$

$\kappa S)(NH_3)_3]^+$. The effect of this simplification on the calculated Mn-N, Mn-C, and C≡O bond distances in $[Mn(CO)_3(tpa-\kappa^3N)]^+$ *vs.* $[Mn(CO)_3(NH_3)_3]^+$ was totally negligible, with absolute individual differences not exceeding 0.04 Å and an average deviation over all parameters of exactly zero. Furthermore, the effect of replacing a κO-bound DMSO by water in the model system also had a negligible effect on the optimized geometry. Mn-N, Mn-C, and C≡O bond distances are virtually identical in both structures and the variation in the Mn-O bond is just 0.06 Å. Therefore, it is not surprising that the C≡O stretches are also calculated to be essentially the same in $[Mn(CO)_2(NH_3)_3(OH_2)]^+$ *vs.* $[Mn(CO)_2(dmso-\kappa O)(NH_3)_3]^+$, with a deviation of only 1 cm^{-1} for the antisymmetrical and 14 cm^{-1} for the symmetrical mode. With the exception of the Mn-O vs. Mn-S bond, $[Mn(CO)_2(dmso-\kappa S)(NH_3)_3]^+$ also gave Mn-N, Mn-C, and C≡O bond distances very similar to the other two dicarbonyl model structures. The symmetrical and antisymmetrical C≡O stretching vibrations showed more significant differences to the aquo and κO-bound DMSO systems though, of about 70–85 cm^{-1}. However, since among the 73 entries in the CSD database (version 5.34) of structurally characterized manganese-DMSO compounds, there is not a single one with the dimethylsulfoxide coordinated via the soft sulfur atom, we conclude that this binding mode is not relevant and thus does not need to be further considered here. In summary, these calculations clearly demonstrate that the modelling of the coordinated solvent by aquo ligands is a valid one, since the replacement of dmso-κO by H_2O has a negligible effect on the calculated bond distances and vibrations. Furthermore, the DMSO solvent was still accounted for at least in the form of the COSMO model.

References

1. Z. Tyeklár, R. R. Jacobson, N. Wei, N. N. Murthy, J. Zubieta and K. D. Karlin, *J. Am. Chem. Soc.*, 1993, **115**, 2677.
2. P. A. Anderson, G. B. Deacon, K. H. Haarmann, F. R. Keene, T. J. Meyer, D. A. Reitsma, B. W. Skelton, G. F. Strouse, N. C. Thomas, J. A. Treadway and A. H. White, *Inorg. Chem.*, 1995, **34**, 6145.